AD-757 655

RADAR SEA RETURN-JOSS II

J. C. Daley, et al

Naval Research Laboratory
Washington, D. C.

21 February 1972

NRL Report 7534

Radar Sea Return—JOSS II

J. C. DALEY, J. T. RANSONE, JR., AND W. T. DAVIS

Radar Division

February 21, 1973

NAVAL RESEARCH LABORATORY
Washington, D.C.

CONTENTS

PREVIOUS REPORTS IN THIS SERIES

"Radar Sea Return—JOSS I," J. C. Daley, J. T. Ransone, and J. A. Burkett, NRL Report 7268, May 11, 1971

Security Classification

DOCUMENT CONTROL DATA - R & D

(Security classification of title, body of abstract and indexing annotation must be entered when the overall report is classified)

1. ORIGINATING ACTIVITY (Corporate author) Naval Research Laboratory Washington, D.C. 20375	2a. REPORT SECURITY CLASSIFICATION Unclassified 2b. GROUP

3. REPORT TITLE

RADAR SEA RETURN—JOSS II

4. DESCRIPTIVE NOTES (Type of report and inclusive dates)

A final report on this phase of the Problem.

5. AUTHOR(S) (First name, middle initial, last name)

J. C. Daley, J. T. Ransone, Jr., and W. T. Davis

6. REPORT DATE	7a. TOTAL NO. OF PAGES	7b. NO. OF REFS
February 21, 1973	20	7

8a. CONTRACT OR GRANT NO. NRL Problem R07-02 b. PROJECT NO. Project WR 0-0167 c. d.	9a. ORIGINATOR'S REPORT NUMBER(S) NRL Report 7534 9b. OTHER REPORT NO(S) (Any other numbers that may be assigned this report)

10. DISTRIBUTION STATEMENT

Approved for public release; distribution unlimited.

11. SUPPLEMENTARY NOTES	12. SPONSORING MILITARY ACTIVITY
	Department of the Navy (Naval Oceanographic Office) Washington, D.C. 20375

13. ABSTRACT

Personnel at the Naval Research Laboratory have conducted a radar sea return measurement program in conjunction with the Joint Ocean Surface Study (JOSS II) sponsored by the Naval Oceanographic Office. The 4FR system was employed to obtain sea return data for various sea conditions as a function of radar wavelength and polarization for depression angles at and near the vertical. The results obtained were incorporated with previous measurements at vertical incidence and compared to recent theoretical predictions. From these results the following conclusions were drawn:

1. The normalized radar cross section at 90° depression angle is inversely proportional to wind velocity and may be estimated by an equation of the form $\sigma_0 \propto U^{-0.6}$ for short wavelengths.
2. Existing models are in agreement with the trend of σ_0 with wind velocity.
3. A better fit to both the wind and wavelength dependence of radar sea return at vertical incidence is obtained when the effect of the antenna pattern is included in the model.

DD FORM 1 NOV 65 1473 (PAGE 1)

S/N 0101-807-6801

Ia

Security Classification

Security Classification

14 KEY WORDS	LINK A		LINK B		LINK C	
	ROLE	WT	ROLE	WT	ROLE	WT
Radar cross sections						
Normalized radar cross sections						
Oceans						
Wind velocity						
Wind direction						
Sea state						
Wave-height spectrum						

IL B

DD FORM 1 NOV 65 1473 (BACK)
(PAGE 2)

Security Classification

RADAR SEA RETURN—JOSS II

INTRODUCTION

Test Sites

As part of a continuing program to investigate the characteristics of radar sea return, personnel of the Naval Research Laboratory have conducted a measurement program off the east coast of the United States. These measurements were made in conjunction with the Joint Ocean Surface Study (JOSS II) sponsored by the Naval Oceanographic Office with the objective of investigating the nature of the sea return at vertical and near-vertical incidence. The NRL 4FR system was utilized to obtain calibrated data in the form of the range-gated amplitude and phase of the sea return. In the course of the program the normalized radar cross section (NRCS) was measured for various sea states as a function of radar wavelength, polarization, and depression angle. Surface truth was acquired at the operating sites from the instrumented buoy XERB 1 and the ocean station vessel, OSV *Hotel,* both of which supplied hourly readings of the wind velocity, direction, and average wave height.

The site locations are shown in Fig. 1 along with a simplified representation of the flight plan. When the aircraft reached XERB 1, radar data were recorded by fixing the antenna depression angle (azimuth along the flight path) and sampling the return over approximately a 30-s period. This procedure was repeated for depression angles of 40°, 50°, 60°, 70°, 80°, 90° in upwind, downwind, and crosswind directions, and at least twice in each direction. The gross surface conditions encountered at each site are listed in Table 1. Most of the measurements

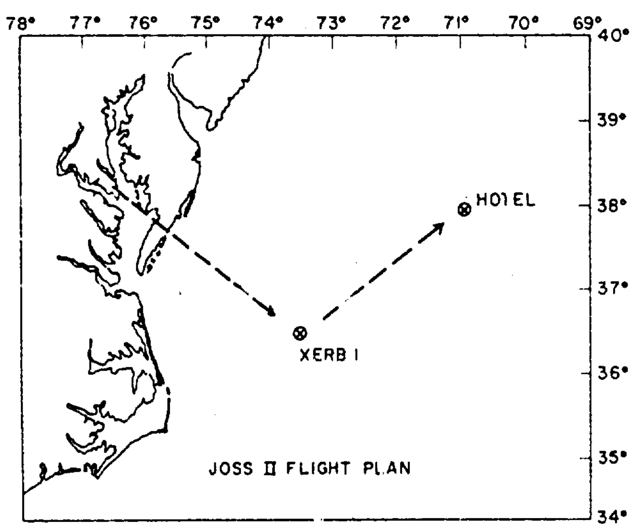

Fig. 1 — JOSS II flight plan

Table 1
Gross Surface Conditions at Buoy XERB 1

Date	Local Time	Wind Velocity (knots)	Average Wave Height (ft)	Depression Angle (deg)
8 Feb 71	1226-1305	14-17	4.4	40-90
	1306-1441	17-29	4.3	40-90
10 Feb 71	1125-1315	24-26	NA	40-90
12 Feb 71	1041-1132	16	NA	40-90
16 Feb 71	1115-1212	13-16	NA	40-90
17 Feb 71	1036-1127	2.5	1.5	40-90
Gross Surface Conditions at Ship: *Hotel*				
8 Feb 71	No 4FR Data	–	–	–
10 Feb 71	1322-1353	28	9.8	40-90
12 Feb 71	No 4FR Data	–	–	–
16 Feb 71	1221-1250	19	4.9	40-90
17 Feb 71	1129-1203	0	0	40-90

were centered around the buoy with only a sampling at each angle at OSV *Hotel*. Hence this report will document the NRCS results obtained at XERB 1 as a function of the radar and surface parameters, and incorporate these results in the context of recent experiment and theory.

The Measurement System

The 4FR system is an airborne coherent pulsed radar capable of transmitting a sequence of four frequencies alternately on horizontal and vertical polarization. These frequencies are X band (8910 MHz), C band (4455 MHz), L band (1228 MHz), and P band/UHF (428 MHz). The details of the system and its absolute calibration by means of reference spheres have been well documented (1). The main characteristics of the 4FR system are given in Table 2. The system allows many choices of pulse repetition frequency (prf), pulse length, i-f bandwidth, and range-gate width. The values used for these parameters during the JOSS II program were prf, 512; pulse length 1.0, μs; i-f bandwidth, 10 MHz; range-gate width, 24 ns.

DATA PROCESSING

The amplitude of radar sea return is best described by its probability distribution. The calculation of the distribution is accomplished through the use of a digital computer which accepts the range-gated samples and is programmed to calibrate the data for all of the desired parameters. The basic outputs of this processing system are cumulative probability distributions of the received power (in decibels) of the 16 possible amplitude components recorded by the 4FR system over the total recording period ($\approx$ 30 s). By means of the sphere measurement, this

Table 2
Four-Frequency Radar System Parameters

Band	Polarization	Azimuth Beamwidth (deg)	Elevation Beamwidth (deg)	Azimuth Minor Lobe (dB)	Elevation Minor Lobe (dB)	Cross Polarization (dB)	Antenna Gain (dB)	Peak Power (kW)	Ave Power (kW)	Pulse Width (μs)	PRF (pps)
P	Horizontal	+12.3	40	14.5	30	25	17.4	25	140	0.25-2.0	100-1463
	Vertical	12.1	41	14.5	26	28	17.4				
L	Horizontal	5.5	13.8	13.4	16	25	25.9	25	140	0.25-2.0	100-1463
	Vertical	5.5	13	14	14	25	26.2				
C	Horizontal	5	5	23.2	24.5	>20	31.4	35	100	0.1-2.0	100-1463
	Vertical	5	5	23.2	24.5	>20	31.4				
X	Horizontal	5	5.3	23.6	23.5	>20	31.2	25	160	0.1-2.0	100-1463
	Vertical	4.7	5.0	23.6	24.2	>20	31.2				

received power may be calibrated in terms of the NRCS. The details of this procedure may be found in previous reports (1,2), with one exception. The illuminated area involved in the definition of the NRCS will be calculated for a two-way antenna pattern rather than the one-way pattern previously used. The effect of this change is detailed in the appendix to this report.

From the distributions obtained, the median value of the NRCS was tabulated for all signal components for each recording run. These values were grouped according to wind direction and depression angle. The median of these sample medians was computed for each surface condition. The results for the direct polarizations are listed in Tables 3-8 with the appropriate wind field and wave height recorded at the buoy during the data-gathering period. No reliable cross-polarization data were obtained. Other omissions in the tables are caused by equipment malfunctions that resulted in lack of reliable data.

Table 3
Median Decibel Values of Normalized Radar Cross Section
Feb. 8, 1971: Wind velocity 14-17 knots; wave height 4.4 ft

Depression Angle (deg)	Wind Direction*	LVV	LHH	PVV	PHH
40°	U	−22	−30	−24	−33.5
	D	−26	−34	−24.5	−35.5
	C	−23.5	−31.5	−21.5	−32
50°	U	−19	−25	−21.5	−27
	D	−21	−26	−20.5	−26
	C	−19.5	−24.5	−20	−24.5
60°	U	−	−	−	−
	D	−16	−19	−15	−19.5
	C	−16	−19.5	−17	−18.5
70°	U	−10.5	−10.5	− 3	− 2
	D	−14	−14	− 4	− 3
	C	−13	−13.5	− 7.5	− 6.5
80°	U	+ 2	+ 2	+ 3.5	+ 2
	D	+ 1	0	+ 3	+ 1.5
	C	− .5	− 1	+ 3.5	+ 3
90°	−	+ 7.5	+ 5.5	+ 1.5	0

*U = upwind, D = downwind, C = crosswind.

Table 4
Median Decibel Values of Normalized Radar Cross Section
Feb. 8, 1971: Wind velocity 17-29 knots; wave height 4.3 ft

Depression Angle (deg)	Wind Direction*	LVV	LHH	PVV	PHH
40°	U	−25	−30.5	−25.5	−34.5
	D	−23.5	−32	−26	−35.5
	C	−25	−32	−23	−31.5
50°	U	−22	−25	−24	−26.5
	D	−20.5	−25	−22.5	−28
	C	−19.5	−25	−21.5	−25
60°	U	−17.5	−18.5	−18.5	−20.5
	D	−15.5	−19	−20.5	N
	C	−16.5	−19.5	−18	−18.5
70°	U	−	−	−	−
	D	−14.5	−13.5	− 9	− 7
	C	−16.5	−13.5	− 3	− 1.5
80°	U		−	−	−
	D	− 3	− 3	+ .5	+ .5
	C	− 2.5	− 1.5	+ 2	+ 1.5
90°	−	+ 5	+ 4.5	+ .5	− .5

*U = upwind, D = downwind, C = crosswind.

Table 5
Median Decibel Values of Normalized Radar Cross Section
Feb. 10, 1971: Wind velocity 24-26 knots; wave height (NA)

Depression Angle (deg)	Wind Direction*	XVV	XHH	CVV	CHH	LVV	LHH	PVV	PHH
40°	U	−19.5	−26	−20.5	−27.5	−25	−32.5	−26.5	−35
	D	−19.5	−26.5	−21.5	−28.5	−25	−32.5	−26.5	−35.5
	C	−24	−30	−25.5	−32	−32.5	−34	−25.5	−34.5
50°	U	−16	−20	−18	−21.5	−24	−28	−24	−29
	D	−15	−19.5	−18.5	−23	−23.5	−28	−24.5	−28.5
	C	−21	−24	−23	−27	−25	−28.5	−24	−29
60°	U	−11	−14.5	−14.5	−15	−21	−24	−18.5	−22.5
	D	−10.5	−14	−15.5	−17	−21	−24.5	−18.5	−21.5
	C	−14	−16.5	−17.5	−18.5	−21.5	−25.5	−18.5	−22.5
70°	U	− 4.5	− 5.5	− 3	− 3.5	−11	−13.5	− 9.5	−12
	D	− 5.5	− 5.5	− 4.5	− 5.5	−10.5	−12.5	− 8.5	− 8
	C	− 5.5	− 5.5	− 3.5	− 4.5	−11	−12.5	− 8.5	− 8
80°	U	+ 2	+ 2	+ 4	+ 3	0	− 2	+ 1.5	+ 1
	D	+ 3.5	+ 3	+ 5.5	+ 4.5	− 1.5	− 4	+ 1	+ 1.5
	C	+ 2.5	+ 2	+ 4	+ 4.5	− 1.5	− 4	+ 1	+ 1
90°	−	+10.5	+ 8	+10.5	+ 9.5	+ 4	+ 1.5	− 1	− 1.5

*U = upwind, D = downwind, C = crosswind.

Table 6
Median Decibel Values of Normalized Radar Cross Section
Feb. 12, 1971: Wind velocity 16 knots; wave height (NA)

Depression Angle (deg)	Wind Direction*	XVV	XHH	CVV	CHH	LVV	LHH	PVV	PHH
40°	U	−26	−31.5	−25	−33	−27	−35.5	−26.5	−39
	D	−27.5	−35	−26	−34.5	−27.5	−36.5	−26	−39
	C	−31.5	−36.5	−29.5	−35.5	−27.5	−37	−27	−40.5
50°	U	−24	−25	−22.5	−27	−25.5	−30	−23.5	−30
	D	−27.5	−30	−23.5	−29.5	−26	−31	−23	−29.5
	C	−29	−31	−25.5	−30.5	−25.5	−30.5	−24	−30.5
60°	U	−19.5	−19	−17.5	−20.5	−23.5	−26	−19.5	−24
	D	−21.5	−21.5	−18.5	−21.5	−23	−26	−19.5	−24.5
	C	−23.5	−23	−20	−23	−23	−26	−18.5	−23.5
70°	U	−8.5	−8	−6	−8.5	−17	−20.5	−12	−13
	D	−9.5	−9	−6.5	−9	−16.5	−20	−11	−13
	C	−9	−8.5	−6	−8	−14.5	−19.5	−11.5	−14.5
80°	U	−2	−.5	+2	+1	−5.5	−6.5	+4.5	+2
	D	+2	+3.5	+5.5	+4.5	−7.5	−8.5	+.5	−1
	C	−1.5	0	+4	+2.5	−6.5	−7	+1	−.5
90°	−	+7.5	+8.5	+11.5	+10.5	+3.5	+1.5	+1.5	−1

*U = upwind, D = downwind, C = crosswind.

Table 7
Median Decibel Values of Normalized Radar Cross Section
Feb. 16, 1971: Wind Velocity 13-16 knots; wave height (NA)

Depression Angle (deg)	Wind Direction*	XVV	CVV	CHH	LVV	LHH	PVV	PHH
40°	U	−21	−22	−30	−26.5	−34.5	−26.5	−37
	D	−20	−22	−30	−26.5	−34.5	−26	−37
	C	−27.5	−26.5	−33.5	−27.5	−35.5	−25	−36.5
50°	U	−16.5	−20.5	−24.5	−25	−30	−24.5	−30.5
	D	−17	−20.5	−25	−24.5	−29	−24	−30
	C	−23	−23.5	−28	−25	−30.5	−22.5	−29
60°	U	−11	−17	−19.5	−22	−25	−18.5	−22.5
	D	−11	−16.5	−19	−21	−24.5	−18	−22.5
	C	−15	−19	−21	−21.5	−25	−17.5	−22
70°	U	− 5.5	− 6.5	− 9	−15	−20	−11	−14
	D	− 6	− 6.5	− 9	−15.5	−20	−12	14
	C	− 8	− 7.5	−10	−15.5	−20.5	−12.5	−16
80°	U	+ 1.5	+ 4.5	+ 3.5	− 5.5	− 6.5	+ 1.5	0
	D	+ 2.5	+ 5	+ 4	− 5.5	− 6.5	+ 1	0
	C	− 1.5	+ 2.5	+ 1	− 7.5	− 9	− 2	2.5
90°	−	+11.5	+10.5	+10	+ 3	+ 1	+ 1.5	1.5

*U = upwind, D = downwind, C = crosswind.

Table 8
Median Decibel Values of Normalized Radar Cross Section
Feb. 17, 1971: Wind velocity 2.5 knots; wave height 1.5 ft

Depression Angle	Wind Direction*	CVV	CHH	LVV	LHH	PVV PHH
40°	U	−28	−32	−27	−32	No good
	D	−27	−30.5	−26	−31	
	C	−34.5	−38	−40.5	N	Transmitter detuned
50°	U	−25	−26	−25	−26	
	D	−25.5	−26.5	−24.5	−26.5	
	C	−27	−29.5	−29.5	−32	
60°	U	−21	−20.5	−21.5	−21.5	
	D	−21	−20	−22	−21.5	
	C	−24	−24	−26.5	−26	
70°	U	− 8.5	−13	−16	−17.5	
	D	− 8.5	−13.5	−16	−17.5	
	C	−13.5	−12	−18.5	−20	
80°	U	+ 1.5	0	−11.5	− 7.5	
	D	+ .5	+ 3	−12.5	−11.5	
	C	0	+ 1.5	−14	−10.5	
90°	−	+11	+12.5	+ 5.5	+ 7.5	

*U = upwind, D = downwind, C = crosswind.

WIND DEPENDENCE OF THE NRCS AT VERTICAL INCIDENCE

The results of JOSS II coupled with previous work (1,2) provide a comprehensive data bank of NRCS measurements at vertical incidence for various surface conditions. To estimate the effect of increasing sea state on the NRCS at vertical, the median wind velocity was determined as a descriptor of increasing sea roughness. Then, the NRCS was plotted as a function of wind for all signal components (Figs. 2-5). Although there is some scatter, the downward trend of the NRCS is evident, especially for the short wavelengths (Figs. 2 and 3). Therefore, a least-squares fit of the relation

$$\sigma_0 \propto U^n \tag{1}$$

was computed, where U is the median wind velocity and the values of n are given in Table 9.

The results of the fit of Eq. (1) are very close with the exception of P-band data; however, recent advances in theory provide an explanation. For comparison with the data, the predicted NRCS are shown in Figs. 2 through 5 as calculated from the models of Barrick (3) and Sledge and George (4). In the Barrick model, based on specular point scattering, the NRCS at vertical incidence is given by

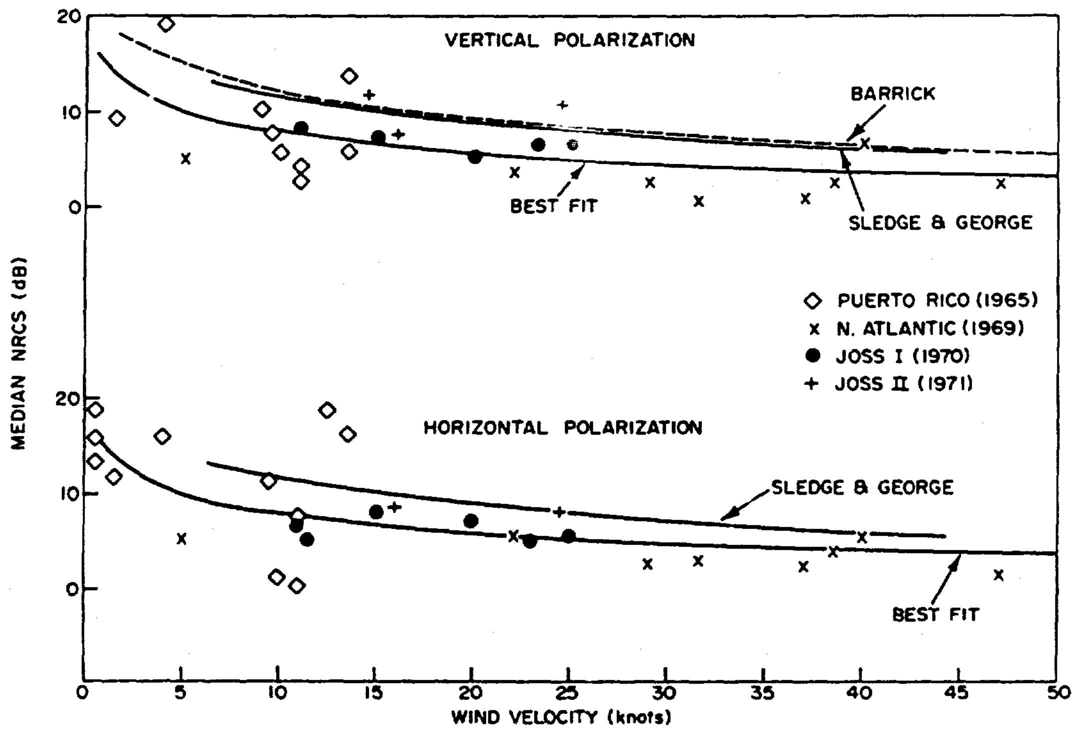

Fig. 2 – Median NRCS vs wind velocity at vertical incidence. X band. Θ = 90°

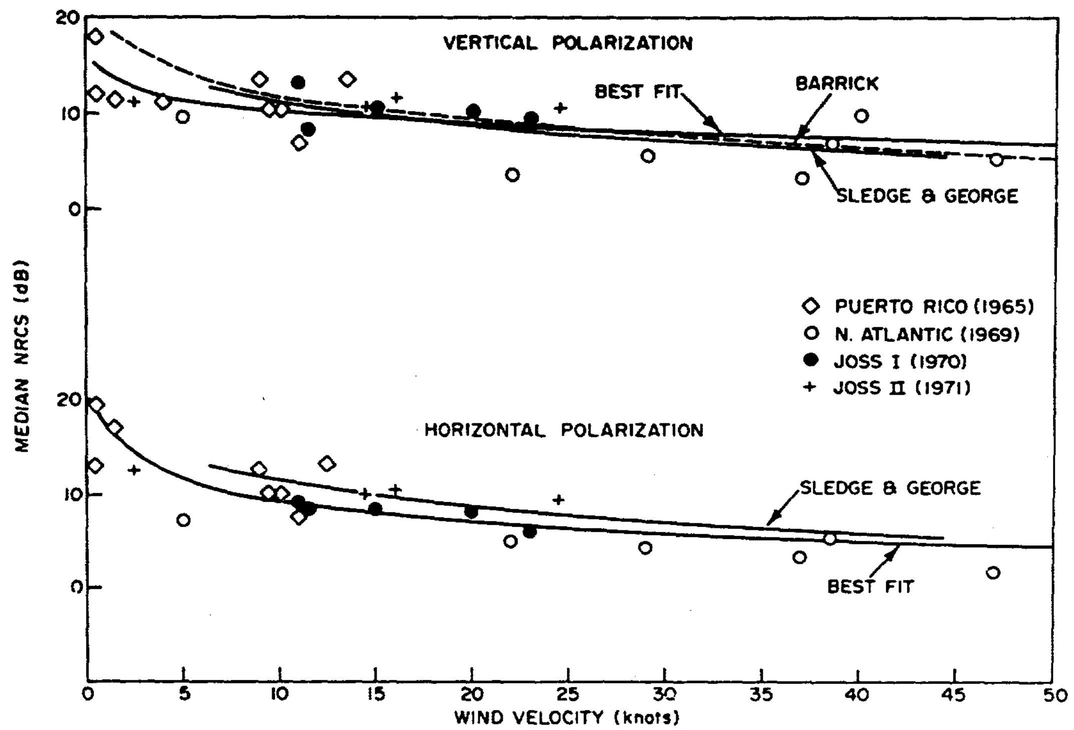

Fig. 3 – Median NRCS vs wind velocity at vertical incidence. C band. Θ = 90°

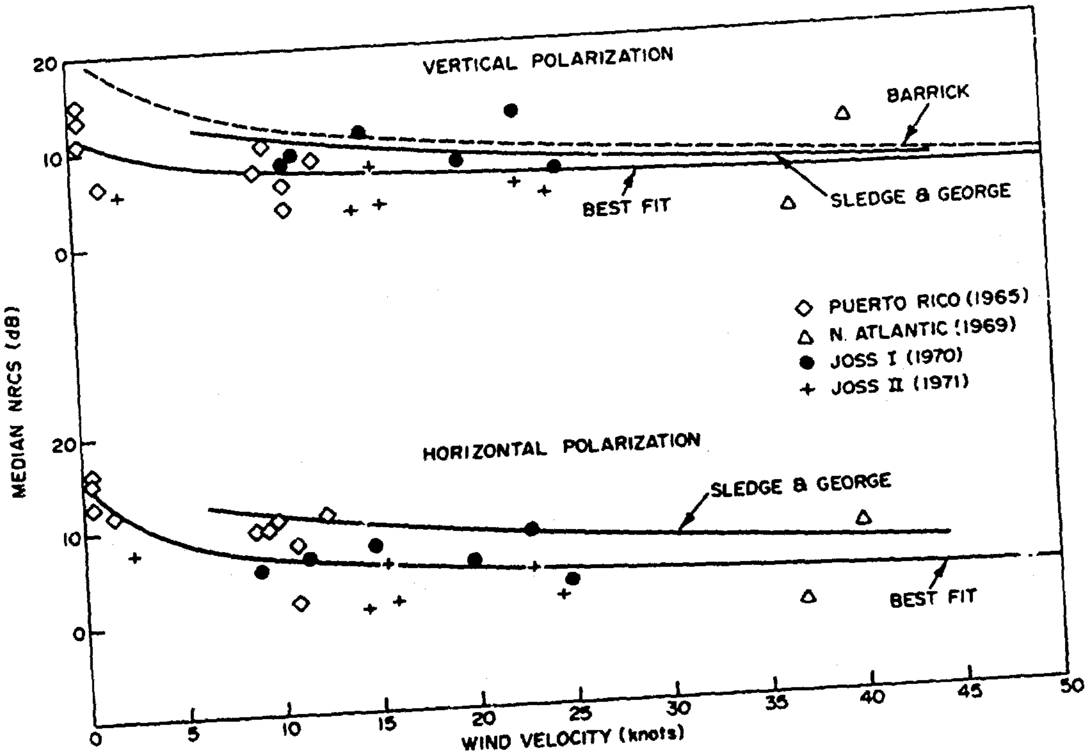

Fig. 4 – Median NRCS vs wind velocity at vertical incidence, L band, $\theta = 90°$

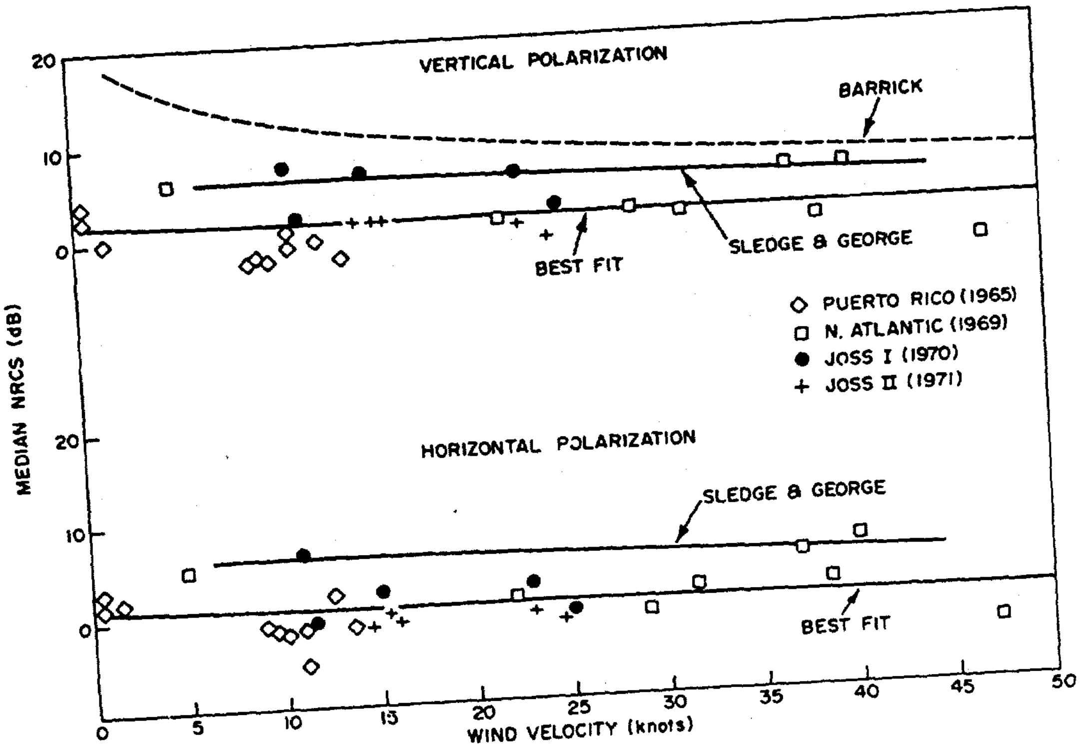

Fig. 5 – Median NRCS vs wind velocity at vertical incidence, P band, $\theta = 90°$

Table 9
Values of n Determined by
Best Fit of $\sigma_0 \propto U^n$

Frequency	Polarization*	
	Vertical	Horizontal
X-Band	−0.6	−0.6
C-Band	−0.4	−0.6
L-Band	−0.3	−0.6
P-Band	−0.0	−0.1

*With limits ±0.1.

$$\sigma_0 = \frac{1}{S^2}|R(0)|^2, \quad (2)$$

where $|R(0)|^2$ is the Fresnel reflection coefficient at vertical incidence and S^2 is the mean square value of the total slope at a point on the two-dimensionally rough surface. The slope can be related to wind velocity as shown by Cox and Munk (5) by

$$S^2 = 0.003 + 5.12\times10^{-3}U, \quad (3)$$

where U is expressed in m/s. The NRCS obtained by combining Eq. (3) with Eq. (2) is shown in Figs. 2-5 and collated with the NRCS obtained experimentally. Although there is some disparity in absolute magnitude, the trend predicted by this model is in good agreement with the X-, C-, and L-band data. Disagreement with the Barrick model exists at P band. This is to be expected inasmuch as Eq. (2) has only a slight dependence on wavelength in the microwave region. However, a better fit to P band is obtained utilizing the model of Sledge and George(4). The model proposed by Sledge and George is nearly equivalent to the Barrick model at the short wavelengths. However, their result involves an integration over the antenna pattern of the radar, and hence introduces a potentially stronger wavelength dependence than Eq. (2). For the 4FR antenna gains the value of the NRCS was calculated from Eq. (A2) of Ref. 4, assuming Cox and Munk statistics (Eq. (3)) and a symmetrical antenna pattern. It is seen in Fig. 5 that a better fit is obtained at P band with the Sledge and George model. Finally, two points should be noted: first, neither model contains an explicit polarization dependence, and hence the theoretical curves of Figs. 2-5 are identical for both vertical and horizontal polarizations. Second, the models compute an average value of NRCS, whereas the data are in terms of the median. So, we have assumed a Rayleigh distribution, and thereby converted the computed averages of the models to median values by the subtraction of 1.6 dB and plotted the predicted median value in the figures. This is a simplifying approximation, as it has been shown that clutter in general is not Rayleigh distributed (6).

SYSTEM LIMITATIONS

Estimated limits of error of the magnitude of the NRCS are provided in Table 10 for each signal component. An additional uncertainty exists at depression angles of 90°. The measurement at 90° (vertical incidence) has inherently a problem of range gating at the center of the

Table 10
Estimated Limits of Error in NRCS (dB)

Date	XVV	XHH	CVV	CHH	LVV	LHH	PVV	PHH
8 Feb 71	–	–	–	–	±2	±1.5	±1.5	±1
10 Feb 71	±2	±1.5	±1	±1.5	±1.5	±2	±2	±1.5
12 Feb 71	±2	±2	±1	±1	±2	±1.5	±2	±2.5
16 Feb 71	±2	–	±1.5	±1.5	±1.5	±2.5	±1.5	±1.5
17 Feb 71	–	–	±2.5	±3	±1.5	±2.5	–	–

antenna beam which is not present at other angles. The specular nature of the return at 90° plus vertical platform motion causes difficulty in continuous range gating at the center of the clutter pile. In these cases, a time history of the return was plotted to test for the presence of large variations in signal produced by poor range gating. Areas of doubtful range gating are then omitted from the compilation of sample medians of the NRCS. (This was also done for previous measurements.) However, it is not possible to determine with certainty whether there was systematic, less-than-optimum, range gating, which would produce a lower NRCS. The problem is not as great at L and P bands due to their larger antenna pattern. However, judging from the agreement with theory of the trend of the NRCS (Figs. 2 and 3), any such uncertainty on X and C bands should be small.

CONCLUSIONS

The processing and analysis of the 4FR radar sea return data recorded in association with JOSS II have been completed. The NRCS from the vertical and horizontal polarizations was determined over depression angles from 40° to 90°. These results were incorporated with previous 4FR sea return data at vertical incidence and compared to recent theory with good results. From the results obtained the following conclusions may be drawn:

1. The NRCS at 90° is inversely proportional to wind velocity and may be estimated by an equation of the form

$$\sigma_0 \propto U^{-0.6}$$

for short wavelengths.

2. The models of Barrick (3) and Sledge and George (4) are in agreement with the trend of σ_0 with wind.

3. The model of Sledge and George provides a good fit to both the wind and wavelength dependence of the NRCS at vertical incidence.

This report completes the documentation of all of the 4FR clutter measurement programs conducted over the past several years. A comprehensive data bank of the variation of sea return as a function of radar and surface parameters has been obtained for depression angles from grazing to vertical incidence, over seas from calm to precipitous. These data have provided and will continue to provide the empirical basis for the development of statistical models of the sea clutter process.

REFERENCES

1. Daley, J. C., Davis. W. T., and Mills, N. R., "Radar Sea Return in High Sea States," NRL Report 7142, Sept. 25, 1970
2. Daley, J. C., Ransone, J. T., Jr., and Burkett, J. A., "Radar Sea Return—JOSS I," NRL Report 7268, May 11, 1971
3. Barrick, D. E., "Rough Surface Scattering Based on the Specular Point Theory" IEEE Trans. Ant. Prop. AP-16 (No. 4), 449-454 (July 1968)
4. Sledge, O.D., and George, S.F., "A Study of Sea Return at Normal and Near-Normal Incidence," NRL Report 7005, Jan. 30, 1970
5. Cox, C., and Munk, W., "Statistics of the Sea Surface Derived from Sun Glitter," J. Mar. Res. 13 (No. 2), 198-227 (1954)
6. Valenzuela, G. R., Laing, M. B., "On the Statistics of Sea Clutter," NRL Report 7349, Dec. 30, 1971

Appendix A

DETERMINATION OF ILLUMINATED AREA

The illuminated area for the pulse-length-limited case was previously approximated (A1) by

$$A = \frac{R\phi a\frac{1}{2}C\tau}{\cos\Theta}, \tag{A1}$$

where ϕa is the azimuth beamwidth of the antenna at the 3-dB point on the one-way pattern and Θ is the depression angle. For the beamwidth-limited case the illuminated area was approximated by

$$A = \frac{R^2\phi a\phi e}{\sin\Theta}, \tag{A2}$$

where ϕe is the elevation beamwidth.

For the 4FR antennas, the patterns on all frequencies are approximately Gaussian, so that

$$\phi' a\,(\text{two-way}) = \frac{\phi a}{\sqrt{2}}$$

and (A3)

$$\phi e'(\text{two-way}) = \frac{\phi e}{\sqrt{2}}.$$

Prior to redefining the illuminated areas for the conditions of Eq. (A3) it will be helpful to examine the derivation of the beamwidth-limited case. A conical beam intersects a plane surface in an ellipse whose area can be determined geometrically. From Figs. A1 and A2, it is possible to write the major and minor axes of the ellipse as

$$Le = h\left[\frac{1}{\tan\left(\Theta - \frac{\phi' e}{2}\right)} - \frac{1}{\tan\left(\Theta + \frac{\phi' e}{2}\right)}\right] \tag{A4}$$

and

$$La = 2R\tan\frac{\phi' a}{2}, \tag{A5}$$

where h = altitude.

The area of the ellipse is given by

$$A = \frac{\pi}{4}LeLa. \tag{A6}$$

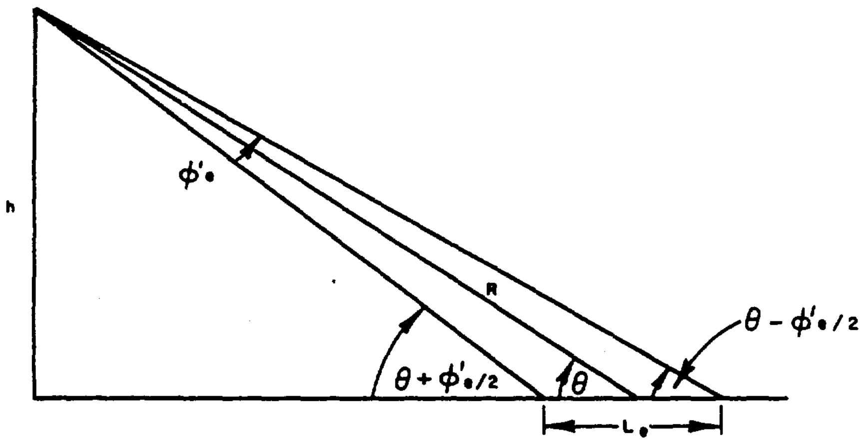

Fig. A1 – Elevation view

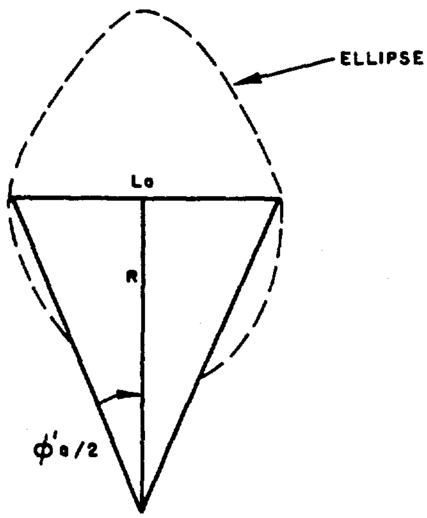

Fig. A2 – Azimuth view

After following substitution of $h = R\sin\Theta$, expanding the tan $(\Theta \pm \phi e'/2)$ terms, and simplifying, Eq. (A6) reduces to

$$A = \frac{\pi}{4} \frac{R^2 \phi' a \phi' e}{\sin\Theta} \tag{A7}$$

when the following approximations are valid:

$$\begin{aligned} \tan \frac{\phi' e}{2} &\approx \frac{\phi' e}{2} \\ \tan \frac{\phi' a}{2} &\approx \frac{\phi' a}{2} \\ \left(\frac{\phi e}{2}\right)^2 &\approx 0. \end{aligned} \tag{A8}$$

Substituting Eq. (A3) into Eqs. (A7) and (A1) results in

$$A = \frac{\pi}{8} \frac{R^2 \phi a \phi e}{\sin\Theta} \text{ (beam limited)} \tag{A9}$$

and

$$A = \frac{R\phi a \frac{1}{2} C\tau}{\sqrt{2}\cos\Theta} \text{ (pulse limited)}$$

where the beamwidths involved are the conventional one-way values as given in Table A Equations (A9) are in agreement with Barton (A2), and a comparison with previous usage (A1) shows that the difference in area is a factor of $\pi/8$ and $1/\sqrt{2}$ for the respective beamwidth and pulse-limited cases. In general, depression angles of 60° and less are pulse limited for the 4FR measurements, so that previously published NRCS values may be converted to the two-way definition by addition of 1.5 dB (pulse limited) and +4 dB (beam limited). The exceptions occur at P band, 90°, where the approximations of Eq. (A8) are not valid and Eq. (A6) must be used. However, the NRCS values may be obtained from Fig. A1.

Table A1
Four-Frequency Radar System Parameters

Band	Polarization	Azimuth Beamwidth (deg)	Elevation Beamwidth (deg)	Azimuth Minor Lobe (dB)	Elevation Minor Lobe (dB)	Cross Polarization (dB)	Antenna Gain (dB)	Peak Power (kW)	Ave Power (kW)	Pulse Width (μs)	PRF (pps)
P	Horizontal	+12.3	40	14.5	30	25	17.4	25	140	0.25-2.0	100-1463
	Vertical	−12.1	41	14.5	26	28	17.4				
L	Horizontal	5.5	13.8	13.4	16	25	25.9	25	140	0.25-2.0	100-1463
	Vertical	5	13	14	14	25	26.2				
C	Horizontal	5	5	23.2	24.5	>20	31.4	35	100	0.1-2.0	100-1463
	Vertical	5	5	23.2	24.5	>20	31.4				
X	Horizontal	5	5.3	23.6	23.5	>20	31.2	25	160	0.1-2.0	100-1463
	Vertical	4.7	5.0	23.6	24.2	>20	31.2				

REFERENCES

A1. Daley, J. C., Davis, W. T., and Mills, N. R., "Radar Sea Return in High Sea States," NRL Report 7142, Sept. 25, 1970

A2. Barton, D. K., *Radar System Analysis,* Prentice-Hall, Englewood Cliffs, N.J., 1964